Electronic Supplementary Material (ESI) for Reaction Chemistry & Engineering.

ELECTRONIC SUPPLMENTARY INFORMATION

Automated separation of immiscible liquids using an optically monitored porous capillary

James H. Bannock[1,2], Tsz Lui[1], Simon T. Turner[1] and John C. deMello[1,2]

[1]Department of Chemistry, Imperial College London,
Exhibition Road, London SW7 2AY, UK

[2]Centre for Organic Electronic Materials, Department of Chemistry,
Norwegian University of Science and Technology, N-7491, Trondheim, Norway

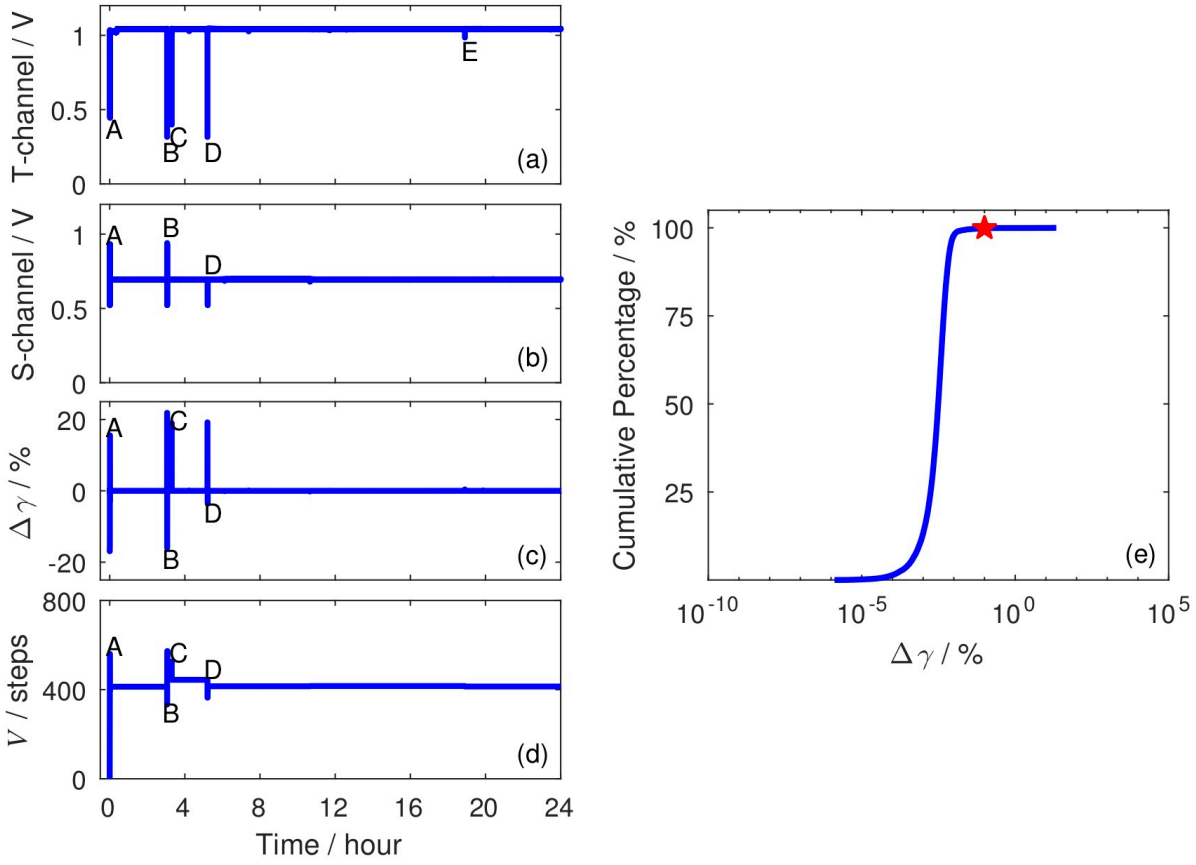

Fig. S1 - Behaviour of automated separator over an extended 24-hour run. Plots showing the T-channel signal (a), the S-channel signal (b), the differential RSD $\Delta\gamma$ (c) and the valve position V (d) versus time, starting from an initial position of $V = 0$ using water and toluene at equal injection rates of 500 μL/min. Following the initial convergence period (marked A in the plots), the S- and T-channel signals remained static for almost the entirety of the run, indicating complete separation. However, short-lived "blips" in the signals occurred at the four points denoted B, C, D and E in the plots, suggesting gas bubbles, dust and/or a temporary loss of complete separation. Re-expressing the time variation of the differential RSD in the form of a cumulative distribution function (e), it can be seen (red star) that $\Delta\gamma$ was smaller than 0.1 % – the empirical criterion for complete separation – for over 99.9 % of the run.

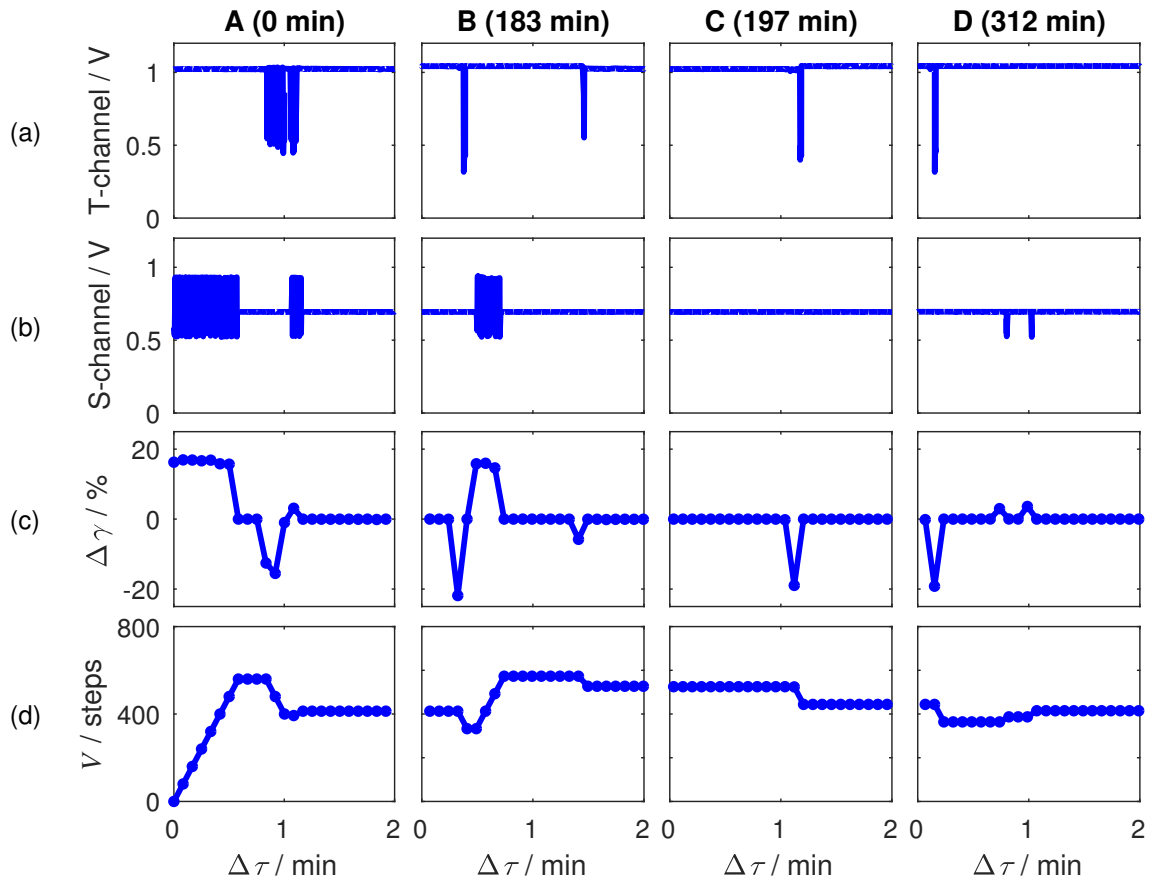

Fig. S2 – Behaviour of separator during the periods of fluctuation identified in Fig. S1. Plots showing the T-channel signal (row a), the S-channel signal (row b), the differential RSD $\Delta\gamma$ (row c) and the valve position V (row d) versus time for the initial convergence phase A and the three "blips" denoted B, C and D in Fig. S1. (The fourth blip denoted E in Fig. S1 corresponded to a single data point in the T-channel transient and was too small to cause any change of the valve position). Initial convergence occurred rapidly, with complete separation being achieved within approximately 70 s of starting the run. The three blips B, C and D were short-lived, with the separator reverting to a state of complete separation within ninety seconds of the initial fluctuation.

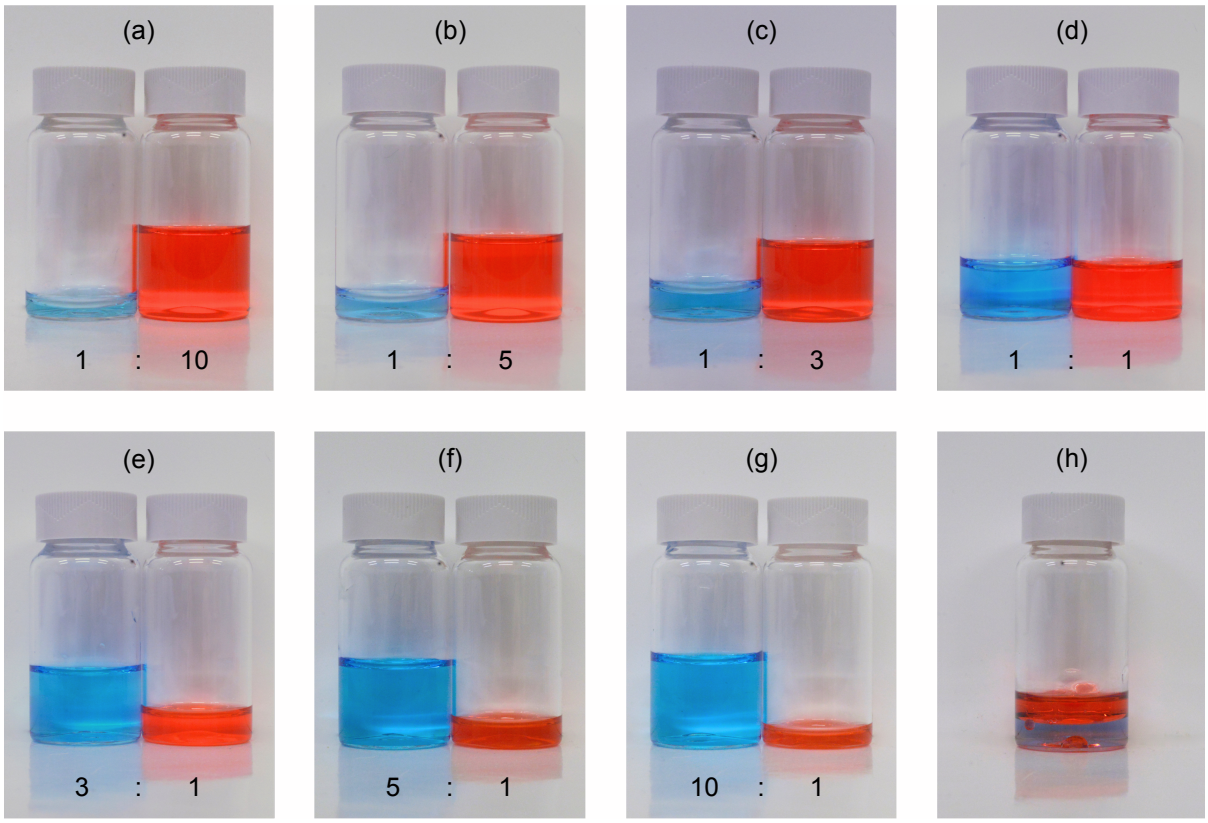

Fig. S3 – Photographs showing vials of water and toluene collected using different water-to-toluene flow-rate ratios in the range 1:10 to 10:1 at a total flow rate of 1 mL/min. The liquids were collected from the two outlets only *after* convergence had been achieved, with water being collected from the T- channel and toluene from the S-channel. For ease of visualization, the water has been dyed blue and the toluene has been dyed orange. There is no evidence of cross-contamination in either channel for any of the flow rates tested (a-g), indicating complete separation of the two liquids. For comparison, a mixed liquid stream obtained under conditions of incomplete separation is shown in (h).

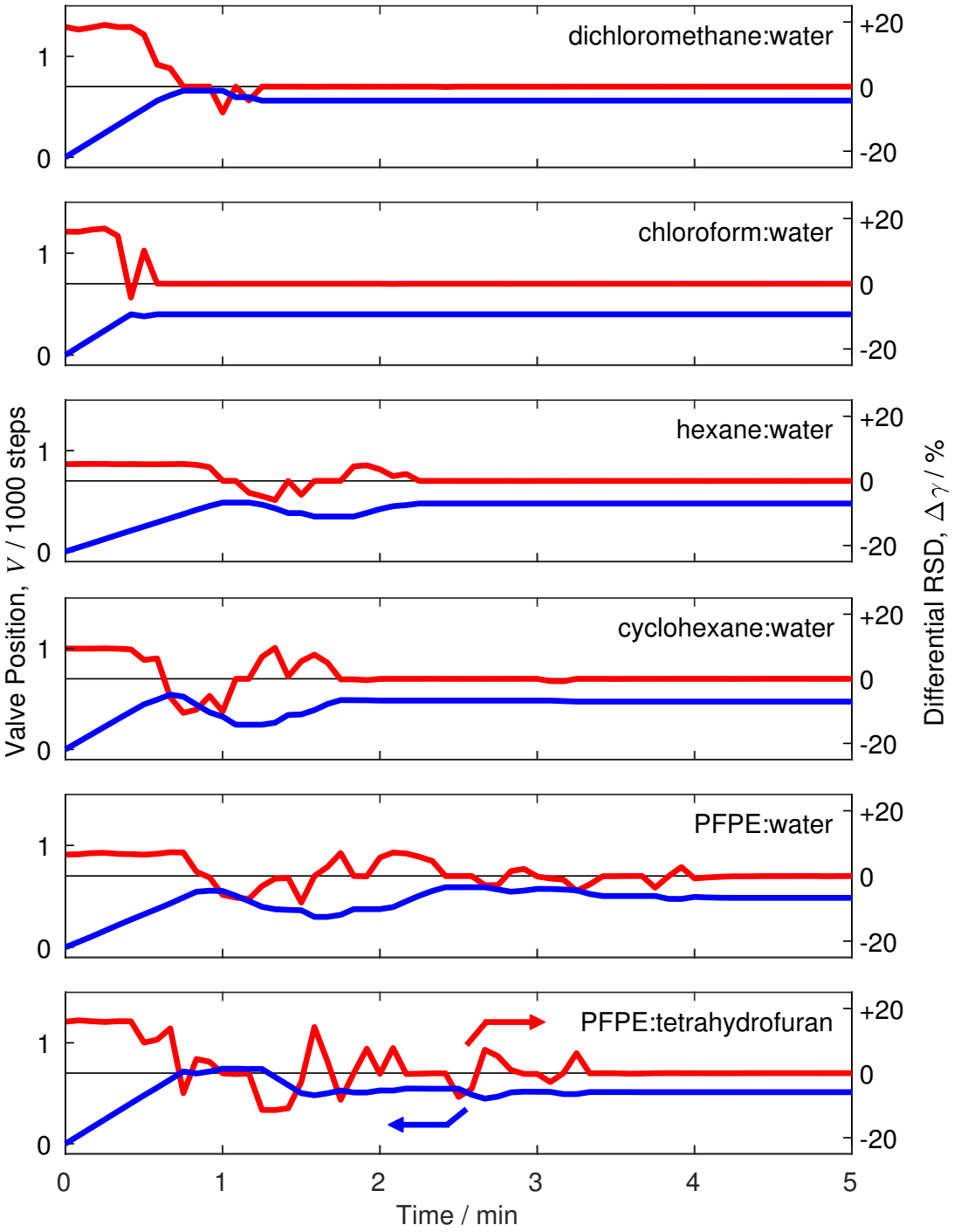

Fig. S4 – Performance of automated separator using various liquid/liquid mixtures at balanced injection rates of 500 μL/min. The plots show the valve position V (blue lines) and the differential RSD $\Delta\gamma$ (red lines) versus time for a variety of aqueous/organic, aqueous/fluorous and organic/fluorous liquid/liquid combinations. The organic/aqueous mixtures converged to a state of complete separation in less than two and a half minutes, with complete separation then being maintained until the end of the five-minute run. Separations involving PFPE required up to four minutes of repeated valve adjustments before converge was reached due to slow (visible) depletion of trapped PFPE from the PTFE jacket (see discussion in main text).

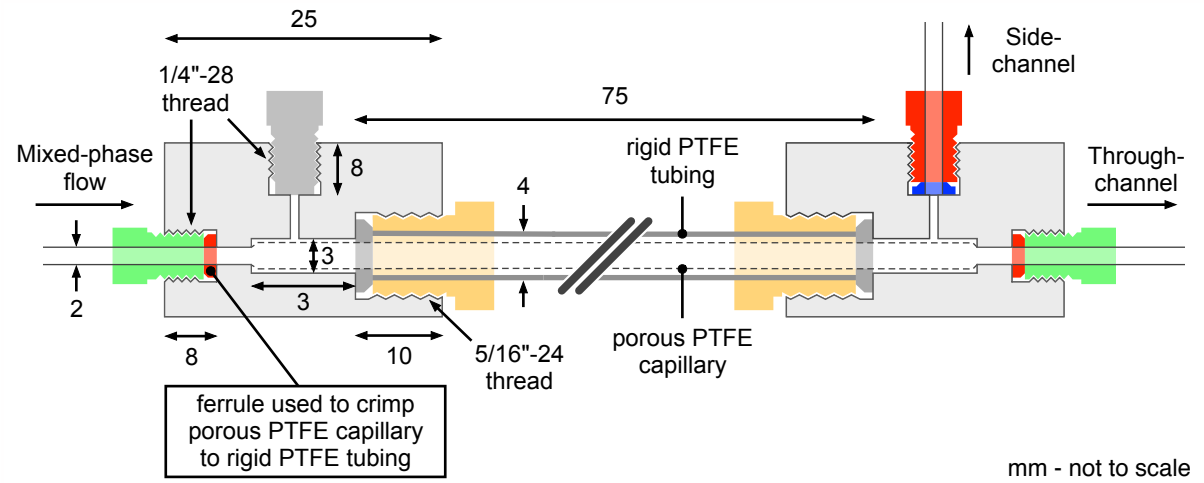

Fig. S5 – Schematic showing a cross-section through the assembled separator. Please refer to Methods section for fabrication details.

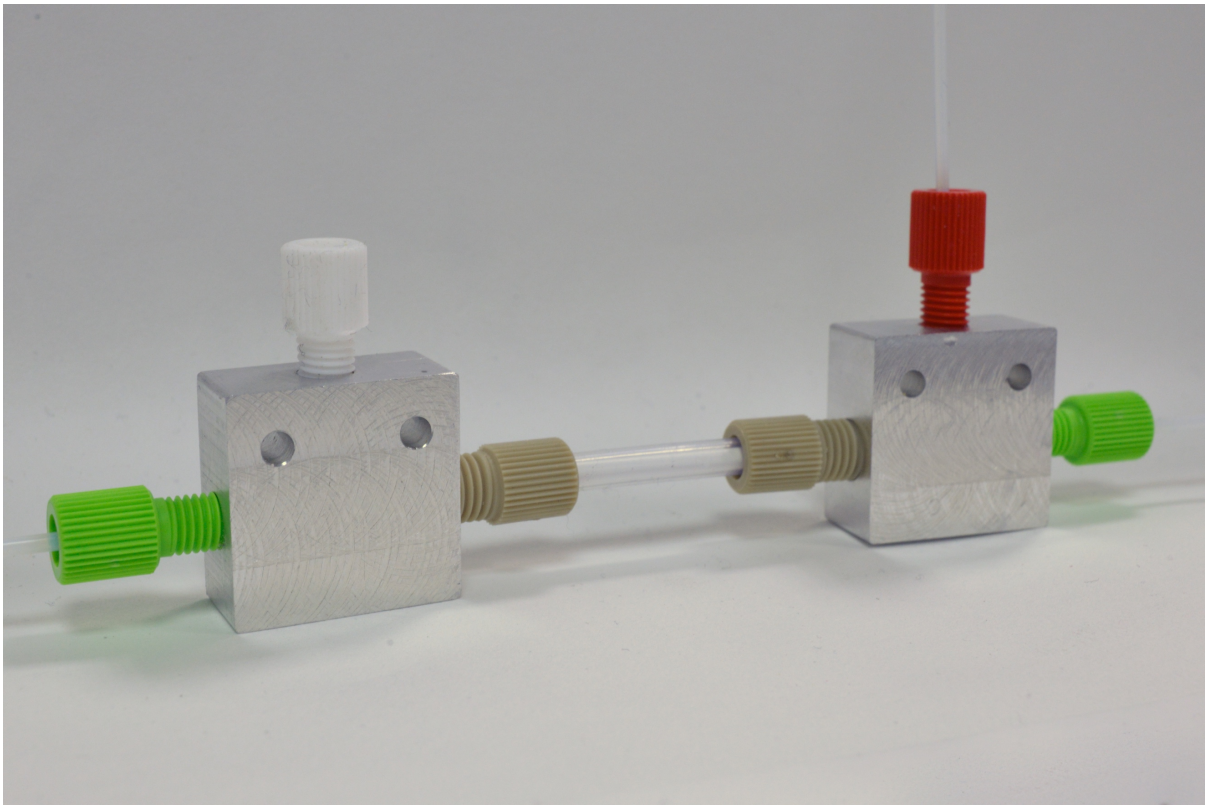

Fig. S6 – Photograph of an assembled jacketed separator. Please refer to Methods section for fabrication details. The terminal blocks shown here were machined from aluminium, while those used for the measurements reported in the paper were machined from PTFE. (The choice of terminal block material was not found to influence the separator performance).

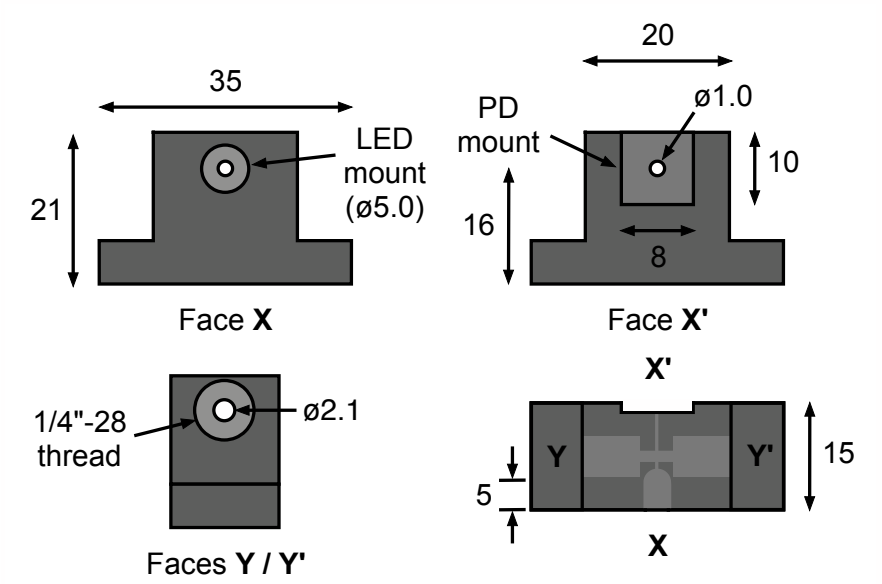

Fig. S7 – Face-on views from various sides of a light emitting diode/ photodiode (LED/PD) 'detection block'. Please refer to Methods section for fabrication details.

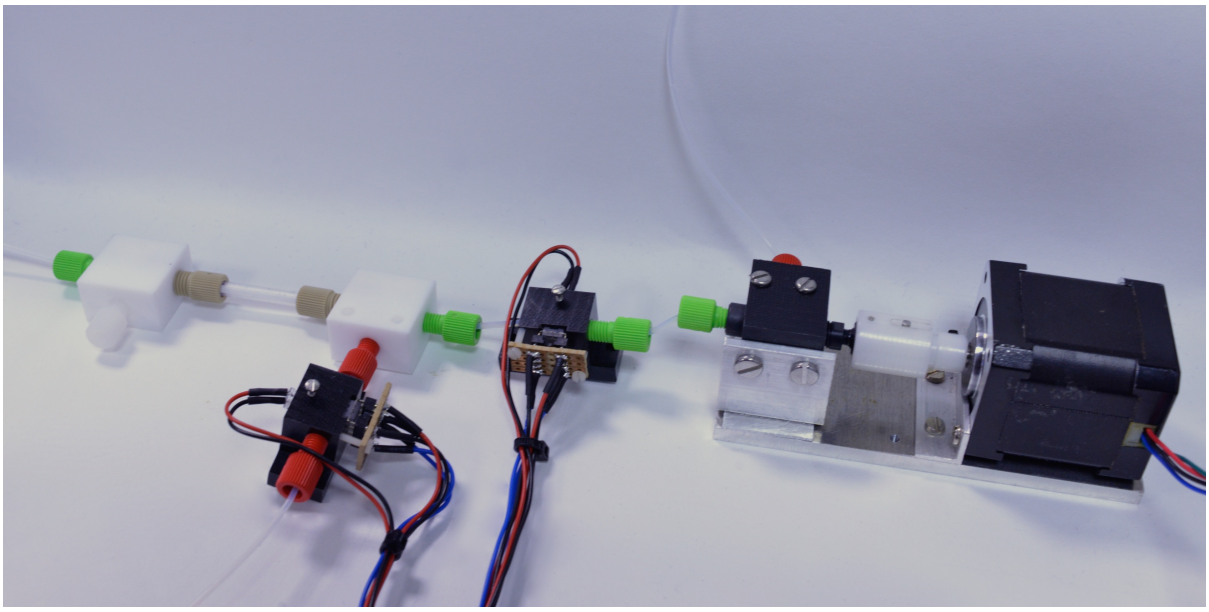

Fig. S8 – Photograph of a fully assembled automated separator, comprising: motorised needle valve, jacketed separator and optical detectors at each outlet. Please refer to Methods section for assembly details.